HYDROLOGICAL PROCESSES
*Hydrol. Process.* **30**, 783–794 (2016)
Published online 20 September 2015 in Wiley Online Library
(wileyonlinelibrary.com) DOI: 10.1002/hyp.10649

# Physically based simulation of the streamflow decrease caused by sediment-trapping dams in the middle Yellow River

Haiyun Shi,[1,2] Tiejian Li,[1*] Kai Wang,[3] Ang Zhang,[1] Guangqian Wang[1] and Xudong Fu[1]

[1] *State Key Laboratory of Hydroscience and Engineering, Tsinghua University, Beijing 100084, China*
[2] *Department of Civil Engineering, The University of Hong Kong, Hong Kong, China*
[3] *China Institute of Water Resources and Hydropower Research, Beijing 100038, China*

## Abstract:

As a result of climate change/variation and its aggravation by human activities over the past several decades, the hydrological conditions in the middle Yellow River in China have dramatically changed, which has led to a sharp decrease of streamflow and the drying up of certain tributaries. This paper simulated and analysed the impact of sediment-trapping dams (STDs, a type of large-sized check dam used to prevent sediment from entering the Yellow River main stem) on hydrological processes, and the study area was located in the 3246 $km^2$ Huangfuchuan River basin. Changes in the hydrological processes were analysed, and periods of natural and disturbed states were defined. Subsequently, the number and distribution of the STDs were determined based on data collected from statistical reports and identified from remote sensing images, and the topological relationships between the STDs and high-resolution river reaches were established. A hydrological model, the digital Yellow River integrated model, was used to simulate the STD impact on the hydrological processes, and the maximum STD impact was evaluated through a comparison between the simulation results with and without the STDs, which revealed that the interception effect of the STDs contributed to the decrease of the streamflow by approximately 39%. This paper also analysed the relationship between the spatial distribution of the STDs and rainfall in the Huangfuchuan River basin and revealed that future soil and water conservation measures should focus on areas with a higher average annual rainfall and higher number of rainstorm hours. © 2015 The Authors Hydrological Processes Published by John Wiley & Sons Ltd.

KEY WORDS digital Yellow River integrated model; human impact; hydrological processes; sediment-trapping dam; Huangfuchuan River basin; middle Yellow River

*Received 16 April 2013; Accepted 13 August 2015*

## INTRODUCTION

Hydrological processes in a river basin can be largely influenced by two key factors: climate change/variation and human activities. Because of the current state of continuous global warming, the impact of climate change on hydrological processes has drawn the attention of numerous researchers. In most river basins, climate change is indeed the dominant factor influencing hydrological processes (Garbrecht *et al*., 2004; Labat *et al*., 2004; Novotny and Stefan, 2007). However, in certain river basins with considerable land-use change, human impacts on hydrological processes could be much greater than the impacts of climate change (Changnon and Demissie, 1996; Mu *et al*., 2007; Shi and Wang, 2015); therefore, human impacts are the more important factors to be elucidated. The quantitative simulation and analysis of human impacts in such river basins have become a key scientific issue in the field of river basin management.

The basin of the middle Yellow River in China is considered to be severely affected by human impacts (e.g. Liang *et al*., 2013; Wang *et al*., 2015). As a semi-arid region, water availability is limited in this basin, whereas water demand is increasing rapidly and continuously because of population growth and economic expansion, accounting for a large proportion of the available water resources. According to available statistics, 65% of the total water volume of the Yellow River was utilized for human purposes from 1986 to 1997 (Xu, 2007). Moreover, because it is a severely eroded region, a substantial number of soil and water conservation measures have been implemented since the late 1950s, and these measures have markedly changed the hydrological conditions and influenced the streamflow in most of the tributaries of the middle Yellow River (Ni *et al*., 1997; Ran *et al*., 2008; Xu and Wang, 2011). It is worth noting that sediment-trapping dams (noted as STDs hereafter), a type of large-sized check dam used to prevent sediment from entering the main stem of the Yellow River, are the most widespread

*Correspondence to: Tiejian Li, State Key Laboratory of Hydroscience and Engineering, Tsinghua University, Beijing, 100084, China.
E-mail: litiejian@tsinghua.edu.cn

structures in this region (Xu *et al*., 2004). Generally, a check dam has a maximum drainage area of 10 acres (0.04 km$^2$) and a maximum height of 2 ft (0.61 m). However, design standards for the drainage area and height of the STDs in this region are no less than 1 km$^2$ and 5 m, respectively (Upper and Middle Yellow River Bureau, YRCC, 2005), which are much larger than those of usual check dams. In addition, the STD structure is usually simplified and does not contain a spill tunnel or spillway, which leads to the complete interception of water and sediment from upstream areas; thus, the STDs are considered to be the most important human impact factor. Overall, the annual runoff in this region has presented a significant decreasing trend over the past several decades that has differed from the general trend of inter-annual variation with climate change and cannot be well explained by climate change alone. Therefore, human impacts must be considered (Xu, 2007; Shi and Wang, 2015).

Several methods have been used to research the human impacts on hydrological processes, including the water balance method (e.g. Wei *et al*., 1999; Wang *et al*., 2009) and the comparative analysis method (e.g. Basic *et al*., 2000; Kang *et al*., 2001). However, these two methods can merely provide the average results over a study area. In recent years, distributed hydrological models have been widely used and have shown success in simulating the human impacts on hydrological processes (e.g. Takken *et al*., 2001; Chi *et al*., 2005; Shi *et al*., 2012a, b). However, because of the high density of STDs, individually incorporating the dams into a hydrological model is difficult unless the model's spatial resolution is high; therefore, basin-scale studies that include analyses of the impact of individual STDs on streamflow decrease have not been published thus far. Because of the large number and pervasive distribution of STDs, this paper simulated the streamflow of a large basin in the middle Yellow River by considering the STDs individually at a high spatial resolution and analysing, for the first time, their impact on streamflow decrease. The paper is organized as follows: the streamflow changes in the studied Huangfuchuan (HFC) River basin of the middle Yellow River are initially analysed, and after determining the number and distribution of the STDs and establishing the topological relationships between the STDs and river reaches, a physically based hydrological model, the digital Yellow River integrated model (DYRIM) (Wang *et al*., 2007, 2015; Li *et al*., 2009a, b), is adopted to evaluate the impact of STDs on the hydrological processes. The results will be useful for managers when evaluating the effects of previously implemented soil and water conservation measures and help them to make better decisions for the future. In addition, the results will be important to the sustainable development of the local societies and economies as well as the ecological systems in such regions.

## STUDY AREA AND RESEARCH DATA

The study area is the HFC River basin at the northern edge of the Loess Plateau (110°18′–111°12′E, 39°12′–39°54′N), which has a drainage area of 3246 km$^2$. The HFC River basin is a semi-arid plateau region with an average annual rainfall of 406 mm that occurs as short-duration, high-intensity rainstorms in the flood season (from June to September) and an average annual potential evapotranspiration that reaches 1500 mm. The surface materials are highly erodible Quaternary loess in the flat upper land and Pisha stone (i.e. unconsolidated coarse sand stone) in the incised slopes and valleys. Grassland, farmland and forestland are the main types of land use in the study area (Ran *et al*., 2003).

There are three hydrologic stations (Huangfu, Shagedu and Changtan) in the HFC River basin (Figure 1). The Huangfu hydrologic station is adjacent to the outlet and controls approximately 98.5% of the total drainage area of the river basin (3199 km$^2$), and the observed hydrologic data at a daily time scale are available from 1954. In addition, there are 14 rainfall stations available in the HFC River basin (Figure 1), and the observed rainfall data at an hourly time scale are available from the year of completion (the earliest is 1976). The hydrologic data (1954–2012) and rainfall data (1976–2012) used for the simulations of the human impact on the hydrological processes are derived from the Hydrological Bureau, Yellow River Conservancy Commission (YRCC), China. Moreover, because STDs are a pervasive form of human activity in the study area, STD data from the YRCC were also collected, which included various attributes (e.g. name, longitude, latitude, year of completion, controlled drainage area and total storage capacity) for each STD.

The sizes of the rainfall and runoff series described in the previous text are markedly different and may influence the results of the trend test. Consequently, an additional two rainfall stations, Dongsheng (1957–2012) and Hequ (1955–2012), were used to generate a longer rainfall series. The rainfall data recorded at these two stations can be downloaded from http://data.cma.gov.cn. The Thiessen polygon method was used to determine the weighting coefficients of Dongsheng and Hequ, which were computed as 0.23 and 0.77, respectively. A new rainfall series for the trend test (1955–2012) can be derived from these two stations, and it is consistent with the runoff series (1954–2012).

## METHODOLOGY

Figure 2 shows the flow chart of the simulation and analysis methods used in this paper. First, the changes and their effects on the hydrological processes are

 

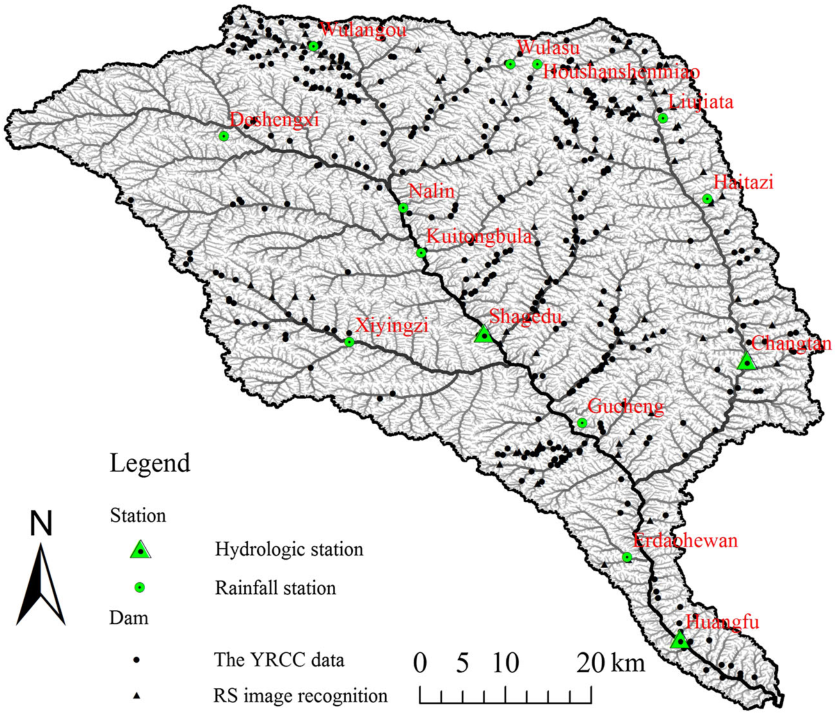


Figure 1. The locations of the stations and distribution of the sediment-trapping dams in the Huangfuchuan River basin. RS, Resources Satellite; YRCC, Yellow River Conservancy Commission

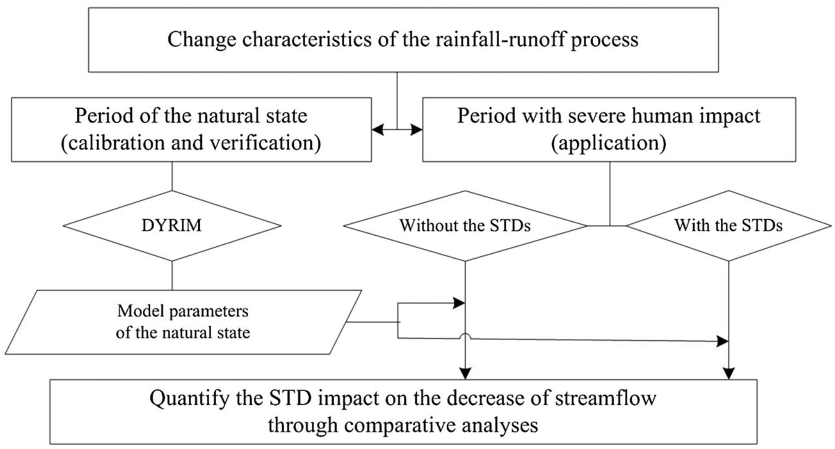


Figure 2. Flow chart of the simulation and analysis methods in this paper. DYRIM, digital Yellow River integrated model; STD, sediment-trapping dam

analysed by using the trend test and change-point test methods, and natural state and disturbed state periods are then defined (the former is for the model calibration and verification, and the latter is for the model application). Second, the number and distribution of the STDs are determined through the data collected from statistical reports and identified from remote sensing images, and the topological relationships between the STDs and river reaches are established. Third, the DYRIM is adopted, and the parameters are then determined by using the observed hydrologic data and rainfall data during the period in a natural state. The remaining inputs are left unchanged, and the hydrological processes that are influenced by the STDs or not during the period of a disturbed state are simulated with the determined parameters. The STD impacts on the hydrological processes are then evaluated through a comparison between the simulation results with the STDs and without the STDs.

*Methods for analysing the changes of the hydrological processes and their causes*

1. Trend test method

The Mann–Kendall trend test is a nonparametric rank-based statistical test that was first proposed by Mann

(1945) and further developed by Kendall (1975), and it is widely used in the fields of meteorology, hydrology and sedimentology (Changnon and Demissie, 1996; Burn and Elnur, 2002; Novotny and Stefan, 2007). Based on the Mann–Kendall trend test method, the slope of the series can be computed by using the Thiel–Sen method (Thiel, 1950; Sen, 1968). Moreover, because the autocorrelation series is not applicable for the Mann–Kendall trend test method, prewhitening (von Storch and Navarra, 1995) is required to eliminate the influence of the autocorrelation.

2. Change point test method

The Pettitt change-point test (Pettitt, 1979) is a nonparametric rank-based test used for the identification of a change point. The series is divided into two subsequences according to the first change point, and additional change points in these subsequences are determined if possible.

### *Identification of the STDs*

The STD data from the YRCC are used to investigate the current situation regarding the STDs in the study area. However, certain STDs may exhibit reduced effectiveness after the passage of years because of sediment deposition, and a portion of the STDs may have been destroyed by extreme floods; moreover, the STDs built in recent years may not be included in the YRCC data. Therefore, the STDs must be identified and considered as effective supplements for the YRCC data. In this study, the STDs are identified by using Google Earth (e.g. GeoEye images) and other remote sensing images (e.g. China–Brazil Earth Resources Satellite) (see Shi and Wang, 2015, for details). Finally, the number and distribution of the STDs in the study area are determined.

### *The DYRIM hydrological model*

The DYRIM is a distributed model platform developed by Tsinghua University for hydrological and sediment simulations in river basins (Wang *et al.*, 2007, 2015; Li *et al.*, 2009a, b). The DYRIM uses a high-resolution digital drainage network that is extracted from a digital elevation model (Bai *et al.*, 2015) and coded using a modified binary tree method (Li *et al.*, 2010) to simulate runoff yield and flow routing on each hillslope–channel unit. Moreover, dynamic parallelisation technology based on sub-basin decomposition has been developed to speed up the simulation (Li *et al.*, 2011; Wang *et al.*, 2011; Wu *et al.*, 2013; Shi *et al.*, 2015).

The DYRIM hydrological model is a physically based distributed model that represents the infiltration-excess runoff yield mechanism. This model uses the hillslope–channel as a basic hydrological unit because of the different hydrological response mechanisms of hillslopes and channels. The runoff yield model is established based on the hillslope unit, where the soil mass is divided into topsoil and subsoil layers. A variety of hydrological processes are simulated, including vegetation interception, evapotranspiration, infiltration-excess runoff on the surface, subsurface flow in these two layers and water exchange between these two layers. Figure 3 shows the relationships between the hydrological processes in the runoff yield model (Li *et al.*, 2009a). There are two types of parameters in the DYRIM hydrological model: (1) invariant parameters that are used to describe the properties of the land use and soil types, influenced by the basic features of the river basin and determined from the literature, fieldwork and prior studies, and (2) adjustable parameters that are calibrated and verified with the observed data.

### *Assessment criteria*

To evaluate the performance of the hydrological simulations by using the DYRIM, two objective functions are used as assessment criteria: the relative error (*RE*) and Nash–Sutcliffe coefficient of efficiency (*NSCE*) (Nash and Sutcliffe, 1970). The equations for computing these two objective functions are given as follows:

$$RE = \left(W_{i,\text{sim}} - W_{i,\text{obs}}\right)/W_{i,\text{obs}} \tag{1}$$

$$NSCE = 1 - \frac{\sum_{i=1}^{N}\left(Q_{i,\text{obs}} - Q_{i,\text{sim}}\right)^2}{\sum_{i=1}^{N}\left(Q_{i,\text{obs}} - \overline{Q}_{\text{obs}}\right)^2} \tag{2}$$

where $W_{i,\text{obs}}$ and $W_{i,\text{sim}}$ are the *i*th observed and simulated annual runoffs ($10^8\,\text{m}^3$), respectively; $Q_{i,\text{obs}}$ and $Q_{i,\text{sim}}$ are the *i*th observed and simulated daily discharges ($\text{m}^3$/s),

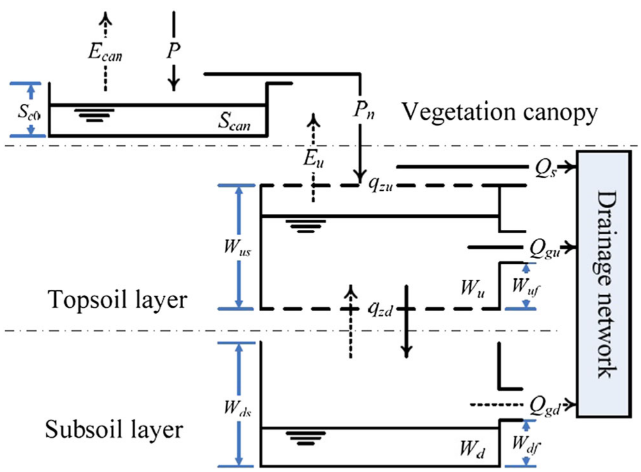


Figure 3. The hillslope hydrological scheme in the digital Yellow River integrated model (Li *et al.*, 2009a)

respectively; $\overline{Q}_{obs}$ is the mean of the observed daily discharge; and $N$ is the sample size.

## RESULTS AND DISCUSSION

*Changes in the hydrological processes*

Based on the observed annual rainfall series (1955–2012) and runoff series (1954–2012), the trend test and change-point test methods were used to investigate changes in the hydrological processes in the HFC River basin. Further comprehensive analyses were conducted to explain the cause. Finally, periods in a natural state and disturbed state with weak or severe human impacts were defined according to the change points.

1. Trends in the rainfall and runoff series

The trends in the rainfall and runoff series were tested by using the Mann–Kendall method and linear regression method, respectively, and the conclusions derived from these two results were consistent. The observed annual rainfall series presented a decreasing trend from 1955 to 2012 that was not significant ($p > 0.1$), whereas the observed annual runoff series presented a marked decreasing trend from 1954 to 2012 ($p < 0.01$). Moreover, the slopes computed by using the Mann–Kendall method were smaller than the slopes computed by using the linear regression method for both the rainfall series and runoff series, and this difference was likely caused by the Mann–Kendall method eliminating the abnormal vibration caused by the external disturbance.

2. Change points in the rainfall and runoff series

The change points in the rainfall and runoff series were tested by using the Pettitt method, which indicated that there was no significant change point in the observed annual rainfall series (1955–2012). The first significant change point for the observed annual runoff series (1954–2012) was found in 1984 ($p < 0.01$), and the second significant change point in the subsequence of the observed annual runoff series (1985–2012) was found in 1998 ($p < 0.05$); no additional change points were found in the other subsequences. As a result, the observed annual runoff series could be divided into three parts: period I (1954–1984), period II (1985–1998) and period III (1999–2012).

3. Comprehensive analyses

As mentioned in our previous study (Shi and Wang, 2015), the cut-off point between the natural state and disturbed state in the HFC River basin based on the results of the present study (i.e. 1984) was inconsistent with the conclusions of prior studies (e.g. Ni *et al*., 1997; Ran *et al*., 2008), which may have been caused by differences in the size of the series used in different studies and the development of society and economy. Furthermore, the average annual runoff in the above three periods decreased in a stepwise fashion, i.e. 57.9 mm in period I, 33.2 mm in period II (57% of the value in period I) and 10.8 mm in period III (19% of the value in period I). However, the average annual rainfall was 437 mm in period I, 397 mm in period II (91% of the value in period I) and 362 mm in period III (83% of the value in period I). Overall, the average annual runoff decreased more rapidly than the average annual rainfall, which indicated that the streamflow decrease may be influenced by factors such as human activities in addition to decreased rainfall. Pervasive STDs had a substantial impact on the hydrological processes in the study area (Xu *et al*., 2004; Mu *et al*., 2007). According to the available statistics, most of the STDs in China were built between the late 1960s and middle 1970s; however, more than 80% were destroyed by extreme flood events that occurred in 1977 and 1978 (Xu *et al*., 2004). A new upsurge in STD construction occurred in the 1980s, and 1118 STDs were constructed from 1986 to 1999 on the Loess Plateau (Feng, 2000). Thereafter, STD constructions starting from 2002 may have had an important impact on the hydrological processes in recent years. The first change point in 1984 may also have been related to the household responsibility system starting in 1979 (Lin, 1992). Under this system, farm lands have been contracted to each family rather than were collectively cultivated in a community level. The families are responsible for their own profits and losses, which led to the high-intensity land use during period II. The second change point in 1998 may also have been related to the policies of the Grain to Green Program and Natural Forest Conservation Program starting in 1999.

In the following sections, period I is regarded as the period of a natural state and is used for the model calibration and verification. Periods II and III are regarded as the periods of a disturbed state with weak and severe human impacts, respectively, and they are used for the model application.

*Digital drainage network and the STDs*

Before performing the simulation, a high-resolution digital drainage network was extracted to provide a suitable spatial discretization scale for running the hydrological model and to establish the topological relationships between the STDs and river reaches. The digital drainage network was extracted with the Advanced

Spaceborne Thermal Emission and Reflection Radiometer Global Digital Elevation Model dataset (30 × 30 m) with the following extraction parameters: critical source area of 1 ha and minimum source channel length of 100 m. Finally, 61 524 river reaches and nearly 154 000 hillslopes were included in the digital drainage network of the HFC River basin (Figure 1).

Known from our previous study (Shi and Wang, 2015), the number of STDs in the HFC River basin was 448, which provided a basic representation of the current situation (Figure 1). The remote sensing-based identification significantly increased the number of STDs because certain small-scale or newly built STDs may not appear in the YRCC data (Figure 4). A full consideration of all of the STDs was an essential prerequisite of the subsequent simulations and analyses. If each STD was built on the nearest river reach of the digital drainage network, the topological relationships between the STDs and river reaches could be established (Figure 5). An example of the various attributes (e.g. ID, longitude, latitude, year of completion, controlled drainage area and the code of the corresponding river reach) recorded at each STD is also shown in Figure 5. Thus, the area controlled by the STDs in the HFC River basin was 1461 km$^2$, which accounted for 45% of the total drainage area.

### *Simulating the impact of STDs on the streamflow decrease*

Water and sediment from upstream locations would be completely intercepted by the STDs if the flood discharge was less than the designed flood discharge (Upper and Middle Yellow River Bureau, YRCC, 2005); in such situations, the runoff yield within the area controlled by the STDs would not contribute to the streamflow observed at the river basin outlet. It is worth noting that this paper focuses on such a situation, and the simulation results represent the maximum STD impact on the hydrological processes.

1. Natural state period

Period I (1954–1984) was regarded as the period in which the processes were in natural state. Because most of the rainfall stations in the HFC River basin were built after 1976, the period from 1976 to 1984 was used for the model calibration and verification. After sorting the observed annual runoff for the nine years (1976–1984) recorded at the Huangfu hydrologic station in ascending order, the 5 years in odd order were used for calibration and the other 4 years were used for verification.

Because of the lack of observation data, the underlying surface of the study area was assumed to be homogeneous. The invariant parameters were determined from the literature and prior studies on the middle Yellow River using the DYRIM, and the adjustable parameters were calibrated and verified with the observed rainfall and hydrologic data. The computational time step and output time step were set at 6 min. The daily discharge and annual runoff were then calculated with the original outputs and compared with the observed data recorded at the Huangfu hydrologic station. Figure 6 shows a comparison of the simulated annual runoff against the observed runoff, and Table I lists the values of relevant assessment criteria of the daily discharge series (using *NSCE*) and annual runoff

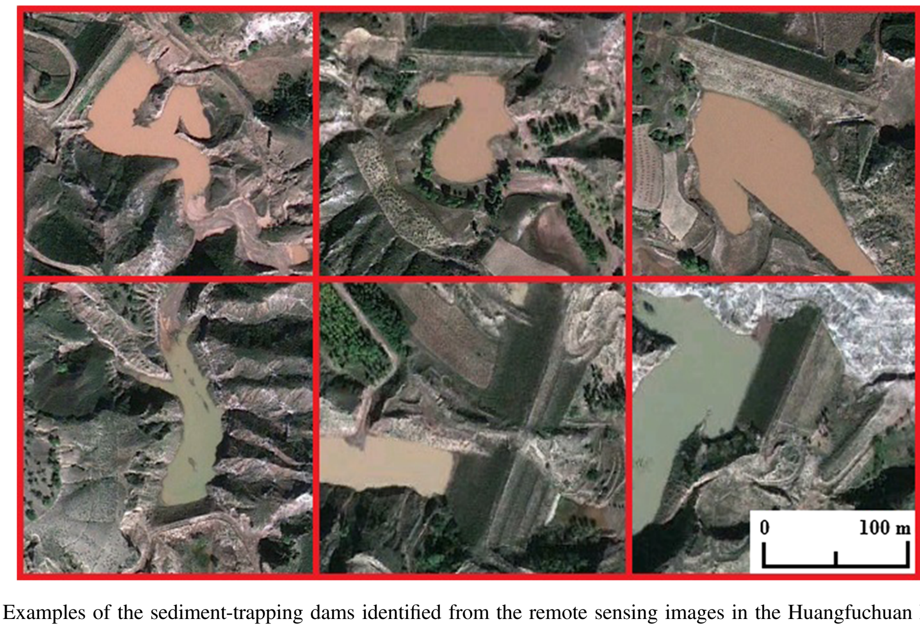


Figure 4. Examples of the sediment-trapping dams identified from the remote sensing images in the Huangfuchuan River basin.

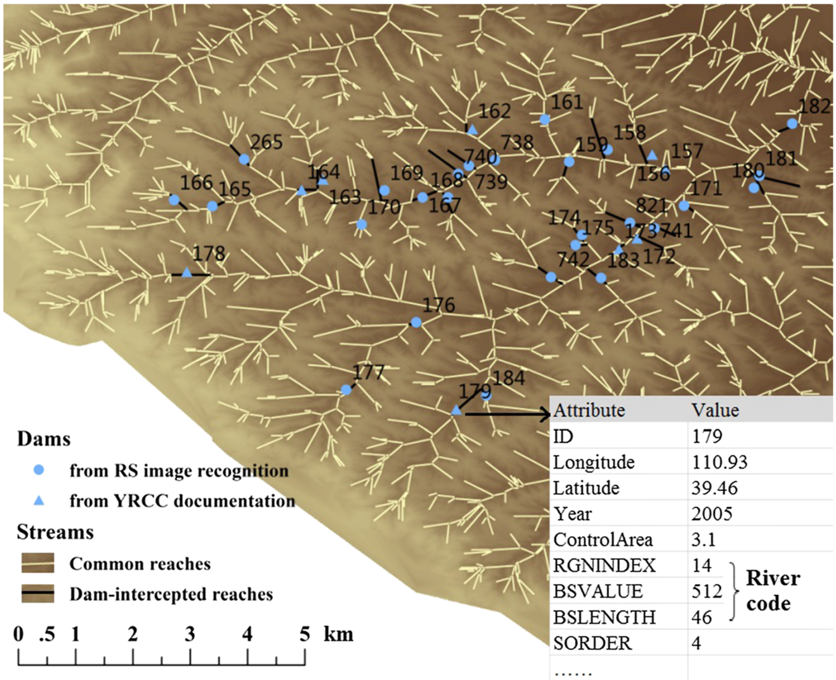


Figure 5. The topological relationships between the sediment-trapping dams and river reaches in the Huangfuchuan River basin. RS, Resources Satellite; YRCC, Yellow River Conservancy Commission

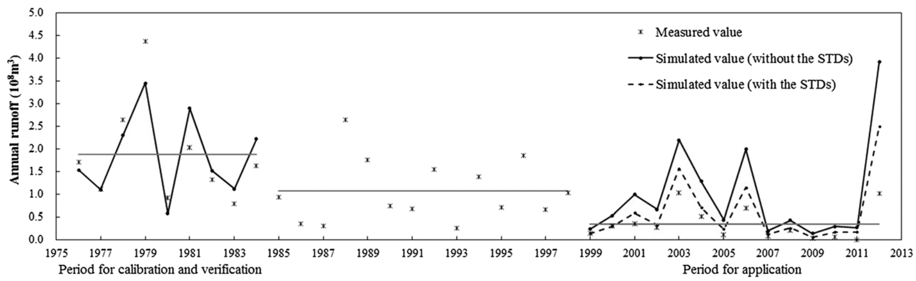


Figure 6. The comparison of the simulated annual runoffs against the observed annual runoffs. STD, sediment-trapping dam

Table I. The *NSCE* and *RE* values during the period of model calibration and verification

| | Calibration | | | | | Verification | | | |
|---|---|---|---|---|---|---|---|---|---|
| Year | 1977 | 1979 | 1981 | 1983 | 1984 | 1976 | 1978 | 1980 | 1982 |
| *NSCE* | 0.27 | 0.95 | 0.42 | 0.28 | 0.43 | 0.57 | 0.82 | −0.5 | 0.69 |
| *RE* (%) | −1 | −21 | 43 | 41 | 36 | −10 | −13 | −37 | 15 |

*NSCE*, Nash–Sutcliffe coefficient of efficiency; *RE*, relative error.

(using *RE*). Overall, the simulated annual runoff was close to the observed values. For the five years of calibration, the *NSCE* values were all greater than 0.25, and a maximum value was found in 1979 (0.95); the *RE* values were all within ±43%, and a minimum value was found in 1977 (−1%). For the four years of verification, the *NSCE* values were greater than 0.57 and *RE* values were within ±15% except for 1980. For 1980, the negative *NSCE* (−0.5) was caused by the discrepancy between the simulated and observed peak floods, and the large *RE* value (−37%) was a result of the spring flood in March and April, which was not simulated by using the DYRIM because the process of snowmelt runoff was not considered in this model.

Consequently, the adjustable parameters were expected to be applicable for the HFC River basin after calibration and verification, and they could be used to simulate the hydrological processes during the period in a disturbed state.

2. Disturbed state periods

Period II and period III were regarded as the periods in a disturbed state with weak and severe human impacts, respectively. Because the STDs used in this paper were identified from recent remote sensing images, the period from 1999 to 2012 was used for simulating the STD impact in the HFC River basin. If the STDs were not considered, then the hydrological processes without the STD impacts could be calculated with the determined parameters. If water from upstream locations was assumed to be completely intercepted by the STDs, then the hydrological processes with the maximum STD impact could be calculated. Figure 6 shows the simulated annual runoff against the observed annual runoff in these two scenarios, and Table II lists the values of relevant assessment criteria. Overall, the simulated annual runoff without the STD impact was much larger than the observed runoff, which indicated that not all of the water in the river basin reached the hydrological station as it did in the natural state, which was most likely a result of the interception effect of the soil and water conservation measures (including the STDs). After considering the STDs in the simulation, the annual runoff for each year decreased markedly and was much closer to the observed runoff than in the simulations that did not include STDs. For the daily runoff series, the negative *NSCE* values without STDs became positive values with STDs except for 2005 and 2012 and the original positive *NSCE* values became higher. This with/without STD comparison indicates that the interception effect of the STDs had a great impact on hydrological processes in the HFC River basin.

Furthermore, the annual runoff during the disturbed period was less than the runoff during the natural period except for the most recent year, 2012, which means that the variation/change in the rainfall pattern (e.g. the proportion of storm rain) was also of importance to the streamflow decrease. However, the STDs and rainfall patterns are not the only reasons for the runoff decrease. The simulated runoff with STDs showed an increasing overestimation during 1999–2012 (Table II and Figure 6), which indicates an increased influence of other factors on the decrease of the observed runoff or an increased number of STDs. However, because of the limited number of STD life data, the influence of STD increments and the influence of other factors cannot be separated in this paper.

Other factors also contributed to the gaps between the simulated and observed runoff. Firstly, the spatial and

Table II. The *NSCE*, *RE* and *IR* values and maximum annual/hourly rainfall during the period of model application (1999–2012)

| Year | | 1999 | 2000 | 2001 | 2002 | 2003 | 2004 | 2005 | 2006 | 2007 | 2008 | 2009 | 2010 | 2011 | 2012 |
|---|---|---|---|---|---|---|---|---|---|---|---|---|---|---|---|
| *NSCE* | (a) | 0.08 | 0.55 | −0.70 | −0.52 | 0.80 | −0.88 | −4.60 | −1.17 | −0.43 | −1.88 | −10.23 | −1.71 | — | −15.06 |
| | (b) | 0.36 | 0.62 | 0.35 | 0.56 | 0.93 | 0.26 | −0.39 | 0.82 | 0.04 | 0.10 | 0.67 | 0.22 | — | −4.64 |
| *RE* (%) | (a) | 63 | 75 | 184 | 144 | 114 | 148 | 316 | 186 | 130 | 111 | 276 | 313 | — | 287 |
| | (b) | −2 | −1 | 71 | 20 | 53 | 36 | 123 | 65 | 46 | 27 | 56 | 145 | — | 147 |
| *IR* (%) | | 40 | 43 | 40 | 51 | 29 | 45 | 46 | 42 | 37 | 40 | 58 | 41 | 37 | 36 |
| Max. annual rainfall (mm) | | 229<br>Haitazi | 243<br>Huangfu | 331<br>Huangfu | 328<br>**Liujiata** | 510<br>Huangfu | 487<br>*Xiyingzi* | 282<br>Kuitongbula | 334<br>*Deshengxi* | 344<br>Huangfu | 491<br>Changtan | 246<br>Huangfu | 214<br>Haitazi | 229<br>Huangfu | 737<br>*Deshengxi* |
| Max. hourly rainfall (mm) | | 26.7<br>Changtan | 37.7<br>**Gucheng** | 43.2<br>*Xiyingzi* | 56.4<br>**Gucheng** | 44.4<br>Changtan | 46.0<br>Kuitongbula | 31.2<br>**Gucheng** | 63.6<br>**Gucheng** | 40.0<br>**Liujiata** | 52.8<br>Changtan | 30.2<br>Shagedu | 33.6<br>**Gucheng** | 33<br>**Liujiata** | 55<br>**Liujiata** |

(a) Without STDs; (b) with STDs. The *NSCE* and *RE* values for 2011 could not be calculated because the observed daily discharge was equal to 0 throughout the year.
*NSCE*, Nash–Sutcliffe coefficient of efficiency; *RE*, relative error; *IR*, impact ratio; STD, sediment-trapping dam.
Stations in bold font indicate high values of the distribution density (DD) of the STDs while stations in italics font indicate low values of the DD.
This table shows an increasing discrepancy of the overestimated discharge, even when the STDs are considered. Thus, the number of STDs is increasing during 1999–2012 or other influences are increasing; however, the cause is not clear because the STD life data are limited.

temporal resolutions of the rainfall data used in this study were not high. The average control area of each rainfall station was approximately 229 $km^2$, and the time intervals between adjacent records were mostly 2 h (or larger), resulting in a negative impact, with short-duration, high-intensity rains possibly being homogenized. As rainfall intensity has been proved to have great impact on streamflow in the middle Yellow River (Luo and Wang, 2013), the low *NSCE* values in calibration and verification periods were mainly caused by the discrepancies between the simulated and observed peak floods. Secondly, as mentioned in the previous text, the spring floods occurred in several years (e.g. 1980 and 1981) could not be simulated by using the DYRIM, which can influence the simulation accuracy to some extent. Thirdly, the parameter uncertainty of the DYRIM is also regarded as an influencing factor of the simulation accuracy. Lastly, other soil and water conservation measures (e.g. farmland terracing and vegetation restoration) were not considered in this paper, and direct water consumptions (e.g. the water abstracted for irrigation, coal mining industry and domestic uses) were difficult to quantify (Li *et al*., 2007; Nakayama, 2011; Shi *et al*., 2012a, 2012b; Liang *et al*., 2013).

*Factors influencing the STD impact*

Table II lists the impact ratios of the STDs (noted as *IR* hereafter, with $IR = 1$ − annual runoff with the STDs/annual runoff without the STDs). The *IR* values fluctuated between 29% and 58% during the period of the model application and presented an inter-annual variation that may have been a result of the differences in the relative positions between the rainfall centres and sub-basins controlled by the STDs in different years. Thus, if the rainfall was mostly centred in the sub-basins controlled by the STDs in one year, additional runoff may have been intercepted by the STDs, and the *IR* value may have been larger; otherwise, the *IR* value may have been smaller. The Thiessen polygon method was used to obtain the control range of each rainfall station, and the distribution density of the STDs (noted as *DD* hereafter) was calculated as the number of STDs within the control range of each rainfall station divided by the control area of corresponding rainfall station. The top three rainfall stations with the highest *DD* were Wulangou (0.35), Liujiata (0.25) and Gucheng (0.24), and the bottom three rainfall stations with the lowest *DD* were Deshengxi (0.037), Erdaohewan (0.059) and Xiyingzi (0.066). Considering the different impacts of the annual rainfall and hourly rainfall on the hydrological processes, these two variables were calculated for each rainfall station for each year from 1999 to 2012. Table II lists the rainfall stations with the maximum annual rainfall or hourly rainfall, with the *DD* of the stations in bold indicating high values and the *DD* of the stations in italics indicating low values. The changes of relative position between the rainfall centres and sub-basins controlled by the STDs in different years were inferred as the main cause of the inter-annual variation of the *IR* values. For example, Liujiata station had the maximum annual rainfall and Gucheng station had the maximum hourly rainfall in 2002; therefore, the *DD* values of these two stations were both large, the hydrological processes were significantly influenced and the *IR* value (51%) was relatively large.

In addition, the average annual runoff during 1999–2012 was $0.59 \times 10^8\,m^3$ and $0.97 \times 10^8\,m^3$ based on the scenarios that considered STDs and those that did not consider STDs, respectively, and the average *IR* value was calculated as 39%, which was slightly lower than the value found for the area proportion controlled by the STDs (45%). The area proportion controlled by the STDs was inferred as a dominant factor for the *IR* value in situations in which the water from upstream was completely intercepted by the STDs; however, other factors may also have had an effect on the *IR* value. For example, because STDs are generally built on common reaches, the runoff yield mechanisms in different parts of the river basin (e.g. main stem and common reaches) may influence the water volume intercepted by the STDs.

*Relationship between the spatial distribution of the STDs and rainfall*

The average annual rainfall of each rainfall station during the period in a disturbed state (1985–2012) and *DD* values within the control range of each rainfall station are listed in Table III. The average annual rainfalls were markedly different, and the highest average annual rainfall (Huangfu station) was 1.8-fold higher than the lowest value (Houshanshenmiao station). All of the rainfall stations were classified into two categories according to the average annual rainfall by using the *K*-means cluster analysis (Table III and Figure 7a), and the examination of significance level $\alpha = 0.01$ was satisfied. Among the four stations with a low average annual rainfall, the *DD* of the Deshengxi and Erdaohewan stations was low, which was explainable, whereas the *DD* of the Houshanshenmiao and Wulangou stations was high. The possible cause of the different values was that rainstorms occurred frequently in the control ranges of the latter two stations and may have resulted in increased soil erosion. Thus, soil and water conservation measures were urgently required. The rainstorm hours (rainfall intensity > 16 mm/h) (China Meteorological Administration, 2013) of each rainfall station from 1985 to 2012 were computed. All of the rainfall stations were classified into two categories according to the rainstorm hours by

 

Table III. The average annual rainfall and distribution density (*DD*) within the control range of each rainfall station during the period in a disturbed state (1985–2012)

| Stations with high average annual rainfall | | | Stations with low average annual rainfall | | |
|---|---|---|---|---|---|
| Station | Average annual rainfall (mm) | *DD* (/km$^2$) | Station | Average annual rainfall (mm) | *DD* (/km$^2$) |
| Huangfu | 361 | 0.14 | Deshengxi | 264 | 0.04 |
| Haitazi | 331 | 0.08 | Erdaohewan | 245 | 0.06 |
| Gucheng | 320 | 0.24 | Wulangou | 232 | 0.35 |
| Shagedu | 319 | 0.14 | Houshanshenmiao | 202 | 0.22 |
| Changtan | 313 | 0.09 | | | |
| Xiyingzi | 297 | 0.07 | | | |
| Kuitongbula | 292 | 0.09 | | | |
| Liujiata | 292 | 0.25 | | | |

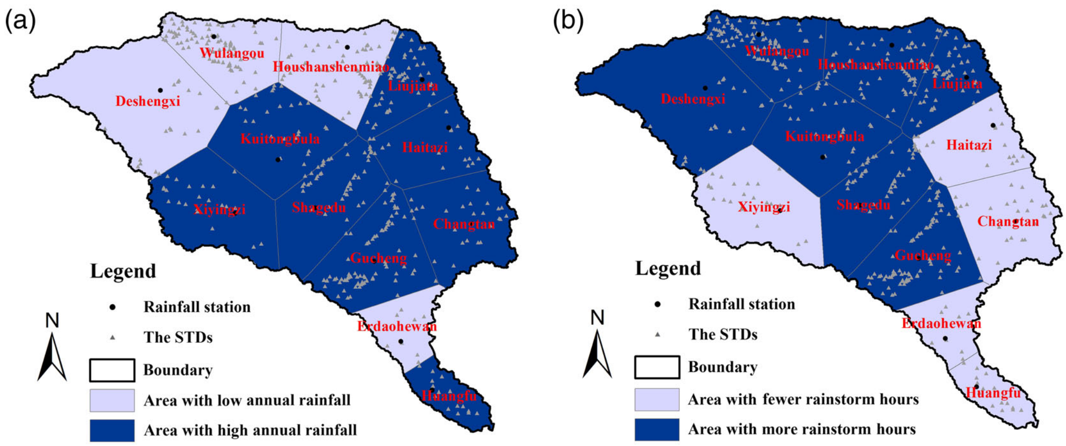


Figure 7. The results of the cluster analysis based on (a) the average annual rainfall and (b) rainstorm hours. STD, sediment-trapping dam

using the *K*-means cluster analysis (Table IV and Figure 7b), and the examination of the significance level $\alpha = 0.01$ was satisfied. Overall, the areas with additional rainstorm hours had a higher *DD* than areas with fewer rainstorm hours. Because the control ranges of the Houshanshenmiao and Wulangou stations were in areas with a greater number of rainstorm hours, the impact of rainstorm hours on the hydrological processes was inferred as a major consideration for STD constructions in such regions in the past. However, certain stations had a high average annual rainfall but few rainstorm hours (Huangfu and Haitazi stations), and the *DD* values were not high.

Therefore, rainstorm frequency is known to be closely related to current STD constructions in the HFC River basin. To improve the management of soil and water loss,

Table IV. The rainstorm hours (rainfall intensity > 16 mm/h) and distribution density (*DD*) within the control range of each rainfall station during the period in a disturbed state (1985–2012)

| Stations with a greater number of rainstorm hours | | | Stations with fewer rainstorm hours | | |
|---|---|---|---|---|---|
| Station | Rainstorm hours (/year) | *DD* (/km$^2$) | Station | Rainstorm hours (/year) | *DD* (/km$^2$) |
| Gucheng | 1.39 | 0.24 | Xiyingzi | 0.37 | 0.07 |
| Liujiata | 0.89 | 0.25 | Changtan | 0.36 | 0.09 |
| Kuitongbula | 0.78 | 0.09 | Huangfu | 0.18 | 0.14 |
| Deshengxi | 0.67 | 0.04 | Haitazi | 0.15 | 0.08 |
| Houshanshenmiao | 0.57 | 0.22 | Erdaohewan | 0.04 | 0.06 |
| Shagedu | 0.55 | 0.14 | | | |
| Wulangou | 0.54 | 0.35 | | | |

 

future soil and water conservation measures should focus on areas with higher average annual rainfall, additional rainstorm hours and lower *DD* (e.g. Shagedu and Kuitongbula stations). In addition, soil and water conservation measures in areas with a high number of rainstorm hours (e.g. Gucheng station) should be further developed.

## CONCLUSIONS

This paper simulated and analysed the impact of STDs on the hydrological processes of the middle Yellow River in China, which is a large region with intensive soil erosion. Using the HFC River basin as the study area, the contribution of this paper can be described as follows.

First, changes to and causes of the hydrological processes in this region were analysed. The annual runoff presented a significant decreasing trend from 1954 to 2012; 1984 was regarded as the cut-off point of the natural state and disturbed state in this region, and 1998 was regarded as the cut-off point of the disturbed state with weak and severe human impacts. The average annual runoff in these three periods (1954–1984, 1985–1998 and 1999–2012) decreased in a stepwise fashion, which was in contrast to the less remarkable decline in the average annual rainfall. Human impact may be a possible cause of this difference.

Second, after determining the number and distribution of the STDs and establishing the topological relationships between the STDs and river reaches, the DYRIM hydrological model was used to physically simulate the STD impact on the hydrological processes. Through a comparison between the simulation results that consider STDs and those that do not consider STDs during the period in a disturbed state with severe human impacts, the maximum STD impact on the hydrological processes in this region was evaluated at 39%. The interception effect of the STDs had a great impact on the hydrological processes, and better results were obtained when the STDs were considered.

This paper also revealed a close relationship between rainstorm frequency and current STD constructions. The conclusions and suggestions proposed in this paper should be useful for managers when evaluating the effects of previous soil and water conservation measures and should help to improve future decision-making.

## ACKNOWLEDGEMENTS

This research was supported by the National Science & Technology Pillar Program in the Twelfth Five-year Plan Period (grant nos. 2012BAB02B02, 2013BAB05B03 and 2013BAB05B05) and the Hong Kong Scholars Program project (grant no. XJ2014059). We are also grateful to the two anonymous reviewers who offered insightful comments that led to improvements of this paper.

## REFERENCES

Bai R, Li TJ, Huang YF, Li JY, Wang GQ. 2015. An efficient and comprehensive method for drainage network extraction from DEM with billions of pixels using a size-balanced binary search tree. *Geomorphology*. DOI:10.1016/j.geomorph.2015.02.028.

Basic F, Kisic I, Butorac A, Nestroy O, Mesic M. 2000. Runoff and soil loss under different tillage methods on Stagnic Luvisols in central Croatia. *Soil & Tillage Research* **62**: 145–151.

Burn DH, Elnur MAH. 2002. Detection of hydrologic trends and variability. *Journal of Hydrology* **255**: 107–122.

Changnon SA, Demissie M. 1996. Detection of changes in streamflow and floods resulting from climate fluctuations and land use-drainage changes. *Climatic Change* **32**: 411–421.

Chi CX, Hao ZH, Wang L, Hu JW. 2005. Study of runoff simulation considering effect of human activity on the Loess Plateau. *Progress in Geography* **24**(3): 101–108 [In Chinese].

China Meteorological Administration. 2013. Rainstorm. [EB/OL]. http://www.cma.gov.cn/ kppd/qxkppdqxcd/201301/t20130109_201593.html. [In Chinese]

Feng G. 2000. The key to bring the Yellow River under control is to speed up construction of check-dams in the Sandy and Grit Areas. *Science and Technology Review* **145**: 53–57 [In Chinese].

Garbrecht J, Van Liew M, Brown GO. 2004. Trends in precipitation, streamflow, and evapotranspiration in the Great Plains of the United States. *Journal of Hydrologic Engineering* **9**(5): 360–367.

Kang SZ, Zhang L, Song XY, Zhang SH, Liu XZ, Liang YL, Zheng SQ. 2001. Runoff and sediment loss responses to rainfall and land use in two agricultural catchments on the Loess Plateau of China. *Hydrological Processes* **15**: 977–988.

Kendall MG. 1975. *Rank Correlation Measures*. Charles Griffin: London; 196.

Labat D, Goddéris Y, Probst JL, Guyot JL. 2004. Evidence for global runoff increase related to climate warming. *Advances in Water Resources* **32**: 631–642.

Li LJ, Zhang L, Wang H, Wang J, Yang JW, Jiang DJ, Li JY, Qin DY. 2007. Assessing the impact of climate variability and human activities on streamflow from the Wuding River basin in China. *Hydrological Processes* **21**: 3485–3491.

Li TJ, Wang GQ, Chen J. 2010. A modified binary tree codification of drainage networks to support complex hydrological models. *Computers & Geosciences* **36**(11): 1427–1435.

Li TJ, Wang GQ, Chen J, Wang H. 2011. Dynamic parallelization of hydrological model simulations. *Environmental Modelling & Software* **26**: 1736–1746.

Li TJ, Wang GQ, Huang YF, Fu XD. 2009a. Modeling the process of hillslope soil erosion in the Loess Plateau. *Journal of Environmental Informatics* **14**(1): 1–10.

Li TJ, Wang GQ, Xue H, Wang K. 2009b. Soil erosion and sediment transport in the gullied Loess Plateau: scale effects and their mechanisms. *Science China Technological Sciences* **52**(5): 1283–1292.

Liang K, Liu CM, Liu XM, Song XF. 2013. Impacts of climate variability and human activity on streamflow decrease in a sediment concentrated region in the middle Yellow River. *Stochastic Environmental Research and Risk Assessment* **27**: 1741–1749.

Lin JY. 1992. Rural reforms and agricultural growth in China. *The American Economic Review* **82**(1): 34–51.

Luo L, Wang ZJ. 2013. Changes in hourly precipitation may explain the sharp reduction of discharge in the middle reach of the Yellow River after 2000. *Frontiers of Environmental Science & Engineering* **7**(5): 756–768.

Mann HB. 1945. Non-parametric tests against trend. *Econometrica* **13**: 245–259.

Mu XM, Zhang L, MVicar TR, Chille B, Gau P. 2007. Analysis of the impact of conservation measures on stream flow regime in catchments of the Loess Plateau, China. *Hydrological Processes* **21**: 2124–2134.

Nakayama T. 2011. Simulation of the effect of irrigation on the hydrologic cycle in the highly cultivated Yellow River basin. *Agricultural and Forest Meteorology* **151**(3): 314–327.

Nash JE, Sutcliffe JV. 1970. River flow forecasting through conceptual models, 1 – a discussion of principles. *Journal of Hydrology* **10**: 282–290.

Ni JR, Han P, Wang GQ, Zhang R. 1997. Variations of sediment characteristics in the middle reach of yellow river with respect to regional water and soil conservations: II. Benefit analysis of reducing the sediment. *Journal of Natural Resources* **12**(2): 126–132 [In Chinese].

Novotny EV, Stefan HG. 2007. Stream flow in Minnesota: indicator of climate change. *Journal of Hydrology* **334**: 319–333.

Pettitt AN. 1979. A non-parametric approach to the change-point problem. *Applied Statistics* **28**(2): 126–135.

Ran DC, Gao JL, Zhao AC, Wang YC. 2003. Analysis on runoff and sediment characteristics and harnessing measure in Huangfuchuan river watershed. *Journal of Hydraulic Engineering* **2**: 122–128 [In Chinese].

Ran DC, Luo QH, Zhou ZH, Wang GQ, Zhang XH. 2008. Sediment retention by check dams in the Hekou-Longmen section of the Yellow River. *International Journal of Sediment Research* **23**: 159–166.

Sen PK. 1968. Estimates of the regression coefficient based on Kendall's tau. *Journal of the American Statistical Association* **63**: 1379–1389.

Shi CX, Zhou YY, Fan XL, Shao WW. 2012a. A study on the annual runoff change and its relationship with water and soil conservation practices and climate change in the middle Yellow River basin. *Catena* **100**: 31–41.

Shi HY, Li TJ, Zhu JF, Zhang A. 2012b. Impact of check dams on the sharp decrease of runoff in the middle Yellow River: case study in the Huangfuchuan River basin. In *The 5th International Yellow River Forum*. Zhengzhou: China; 461–462.

Shi HY, Li TJ, Liu RH, Chen J, Li JY, Zhang A, Wang GQ. 2015. A service-oriented architecture for ensemble flood forecast from numerical weather prediction. *Journal of Hydrology*. DOI:10.1016/j.jhydrol.2015.05.056.

Shi HY, Wang GQ. 2015. Impacts of climate change and hydraulic structures on runoff and sediment discharge in the middle Yellow River. *Hydrological Processes*. DOI:10.1002/hyp.10439.

Takken I, Govers G, Jetten V, Nachtergaele J, Steegen A, Poesen J. 2001. Effects of tillage on runoff and erosion patterns. *Soil & Tillage Research* **61**: 55–60.

Thiel H. 1950. A rank-invariant method of linear and polynomial regression analysis, III. *Proceedings of Koninalijke Nederlandse Akademie van Weinenschatpen* **53**: 1397–1412.

Upper and Middle Yellow River Bureau, YRCC. 2005. *Overview of Sediment Trapping Dams*. China Planning Press: Beijing [In Chinese].

von Storch H, Navarra A. 1995. *Analysis of Climate Variability: Applications of Statistical Techniques*. Springer-Verlag: Berlin; 11–26.

Wang GQ, Fu XD, Shi HY, Li TJ. 2015. Watershed sediment dynamics and modeling: a watershed modeling system for yellow river. In *Advances in Water Resources Engineering, Handbook of Environmental Engineering, Volume 14*, Yang CT, Wang LK (eds). Springer International Publishing: Switzerland: Cham - Heidelberg - New York - Dordrecht - London; 1–40.

Wang GQ, Wu BS, Li TJ. 2007. Digital Yellow River model. *Journal of Hydro-Environment Research* **1**: 1–11.

Wang GS, Xia J, Chen J. 2009. Quantification of effects of climate variations and human activities on runoff by a monthly water balance model: a case study of the Chaobai River basin in northern China. *Water Resources Research* **45**: W00A11.

Wang H, Fu XD, Wang GQ, Li TJ, Gao J. 2011. A common parallel computing framework for modeling hydrological processes of river basins. *Parallel Computing* **37**: 302–315.

Wei T, Zhu J, Zhang X. 1999. Soil water balance of protection forest in the Loess Plateau. *Forestry Studies in China* **1**(2): 47–53.

Wu YP, Li TJ, Sun LQ, Chen J. 2013. Parallelization of a hydrological model using the message passing interface. *Environmental Modelling & Software* **43**: 124–132.

Xu JX. 2007. Impact of human activities on the stream flow of Yellow River. *Advances in Water Science* **18**(5): 648–655 [In Chinese].

Xu JX, Wang HB. 2011. Influence of soil and water conservation measures on reducing in frequency of hyperconcentrated flows in the Wudinghe River basin. *Environmental Earth Sciences* **62**: 1513–1520.

Xu XZ, Zhang HW, Zhang OY. 2004. Development of check-dam systems in gullies on the Loess Plateau, China. *Environmental Science & Policy* **7**: 79–86.


 